Experimental Mechanics (2007) 47:637–648
DOI 10.1007/s11340-006-9032-6

Measurement of the Apparent Density of Green Ceramic Tiles by a Non-contact Ultrasonic Method

G.M. Revel

Received: 18 July 2006 / Accepted: 22 December 2006 / Published online: 6 March 2007

Abstract This paper discusses the problem of the measurement of the apparent density of green ceramic tiles during production. This is a fundamental parameter for the quality of the final product. In fact, the apparent density determines the entity of the dimensional shrinkage of the ceramic body during the firing of tiles, and it is proportional to the final mechanical resistance. Currently, non-destructive systems for the on-line measurement of this parameter are not available. The work presents an innovative method for non-intrusive measurement of the apparent density of green ceramic tiles during the production stage. This method uses non-contact ultrasonic probes. The time of flight of ultrasonic waves is measured during the transmission through the tile. From the time of flight, with the distance between probes known, the propagation velocity can be achieved, which is proportional to the apparent density. The conversion factor between velocity and apparent density is determined by a calibration procedure with a reference method of known uncertainty, e.g. based on a hydrostatic weighing in a mercury bath. This experimental procedure is extensively validated in the work and supported by a theoretical model. The paper presents the theory on which this measurement method lays and the instrumental apparatus, and discusses in detail the analysis of uncertainty. In the end, the paper presents the results of an on-line application.

Keywords Apparent density · Non-contact ultrasonics · Green ceramic tiles · Measurement uncertainty · Non-destructive testing

Nomenclature

ρ	Apparent density
ρ_s	Average actual density
m	Mass
V_a	Apparent volume (pores included)
V_s	Skeleton volume
p	Porosity (%)
v	Longitudinal wave velocity
v_t	Transversal wave velocity
v_a	Sound velocity in air
t_c	Total time of flight through tile and air
T	Air temperature (°C)
$u(x)$	Standard uncertainty of quantity x
u_s	Type A standard uncertainty
u_a	Standard uncertainty evaluated as half-width of a rectangular distribution (Type B)
S_ρ	Standard deviation of ρ achieved by least-squares linear interpolation of the experimental data over the whole considered range
SNR	Signal-to-noise ratio
E	Young's modulus of the porous body
G	Elasticity tangential modulus of the porous body
μ	Poisson coefficient
E_0	Young's modulus at null porosity
G_0	Elasticity tangential modulus at null porosity
b	Empiric parameter proposed by Spriggs [11]
D	Distance between the probes
d_m	Tile thickness
t_a	Time of flight in air without the tile
t_m	Time of flight through the tile thickness
θ	Air relative humidity (%)
$r(t_m,\ t_c)$	Correlation coefficient between t_m and t_c
c_j	Sensitivity coefficients for quantity x_j

G.M. Revel (✉)
Dipartimento di Meccanica, Università Politecnica delle Marche,
Via Brecce Bianche, 60131 Ancona, Italy
e-mail: gm.revel@mm.univpm.it

Introduction

This paper discusses the development and analysis of an innovative non-contact measurement system of the apparent density of green ceramic tiles during the production stage.

The apparent density ρ of a porous body (as a ceramic material) is expressed in kg/m^3 and defined as [1]:

$$\rho = \frac{m}{V_a} \tag{1}$$

where m is the mass and V_a is the apparent (bulk) volume of the body gross open and closed pores, considered as the total volume in the macroscopic external surface of the body, i.e. in its envelope.

On the contrary, the average actual density ρ_s, expressed in kg/m^3, is defined as:

$$\rho_s = \frac{m}{V_s} \tag{2}$$

where V_s is the effective volume of the body net of the closed and open pores. This volume, called skeleton volume, can be obtained grinding the body until it becomes thin powder and then measuring the powder volume.

Therefore, the volume $(V_a - V_s)$ represents the volume of the air in the pores inside the material. The porosity p is thus defined as:

$$p = \frac{\rho_s - \rho}{\rho_s} = \frac{V_a - V_s}{V_a} \tag{3}$$

generally expressed in percentage.

The apparent density of the green tile (not fired but pressed) is a parameter of fundamental importance for the final quality of the ceramic tile [2], as they are made of an aggregate material with pores and granules. As a matter of fact, if the spatial uniformity of this quantity is not adequate, a non-homogeneous shrinkage of the tile will be generated during the firing, causing a dimensional non-conformity, such as irregular shapes, bending and non-constant side length. Moreover, the mechanical resistance of green and fired tiles is proportional to the apparent density.

If raw materials and production parameters are not varied, the apparent density generally remains constant within the desired limits in a production batch. Anyway, in some cases, ρ may have important variations depending on the humidity and the granulometry of the ceramic powder to be pressed and obtained by spray drying. In particular, the powder humidity is the most critical parameter, as it influences the compaction capacity. During production, the powder humidity and particle size may have significant variations (e.g. humidity can change from 4 to 5%) because of uncontrolled variations in the processes before the pressing (e.g. spray drying) or of the long period of storage of the powder into the silo. On the contrary, defects in the spatial uniformity of the apparent density of the single tile can be caused by problems during the automatic feeding of the powder in the press or caused by local wear in the dies.

The apparent density of pressed tiles has a value that, depending on the raw materials and production parameters, can generally change between 1,800 and 2,200 kg/m^3 (with a porosity between 20 and 40%). Nevertheless, for a certain type of production, the apparent density variations to be measured (both as spatial gradient on the single tile body, and as from tile to tile, caused by errors of humidity, particle size or feeding) are very low, normally between 30 and 40 kg/m^3. A difference of apparent density of ±50 kg/m^3 leads to a shrinkage difference of ±0.25% (e.g. 1.1 mm for a tile size of 45×45 cm) on the fired tile caused by non-homogeneous shrinkage.

Moreover, the density sensitivity to the pressure level is very low. In fact, an apparent density variation of 3% (e.g. from 1,980 to 2,040 kg/m^3) is obtained with a pressure variation of 40% (e.g. from 250 to 400 bar). These conditions ask for accuracy in the measurement of ρ in industrial setting of around ±10–15 kg/m^3, equivalent to ±0.50–0.75% of the value.

Despite the need to control this quantity in real time on 100% of the production immediately after the pressing, the state of the art is that no such measurement is done on line. The apparent density can be currently measured off-line in the laboratory (e.g. [3]), and the most used method is generally the hydrostatic weighing in a mercury bath [4], which is based on the measurement of the mass and the estimation of the volume through the measurement of the floating force when the sample bathes. This method allows a good repeatability around ±2 kg/m^3. Mercury represents the ideal fluid for this kind of measure because it has a low specific weight and it does not wet the green tile sample, which would, for example, melt with water.

Nevertheless, mercury is noxious, and it is rarely used in the field to comply with standards (as ISO 14000) regarding environment, safety and health in workplace. Consequently, the apparent density is rarely measured. Moreover, to determine the spatial distribution of the density, it is necessary to cut the tile in pieces and to measure each piece.

Alternative methods for this measure have been proposed in [5–7]. For example, some methods use water instead of mercury, but the piece must be sealed with a coat of paraffin. Other methods use compressed air: the volume is determined through the measurement of the pressure increase in a test chamber with compressed air when the sample is put inside it. The pressure variation (with respect to the test chamber without the sample) is proportional to the volume of the sample. Recently, laser triangulation sensors have been used to measure the volume by a non-contact scanning of the shape.

Nevertheless, these methods do not satisfy industrial needs because they cannot be applied in production line.

Therefore, currently, it is not possible to measure the apparent density during production.

This paper proposes a measurement system based on non-contact ultrasonic transducers for the indirect measure

of the apparent density, through the measurement of the propagation velocity of the waves in the medium.

Since a long time ago, ultrasound sensors are used for the characterization of material properties; nevertheless, the need of contact (through water, gel, etc.) between the probe and the sample limited the application in-line, where the object is often in movement and cannot be touched.

For few years now, probes with high efficiency and sensitivity have been developed, allowing work in non contact mode [8]. These probes could significantly widen the use of ultrasound techniques; nevertheless, it is necessary to assess the measurement uncertainty because of the strong reduction of the signal-to-noise ratio (SNR) produced at the interface between mediums with very different impedances (e.g. air–solid).

In this approach, the time of flight of the ultrasound waves is measured in transmission through the tile. From the time of flight, knowing the distance between the probes, the propagation velocity can be obtained, which is proportional to the apparent density for a given humidity level.

Thanks to the non-contact measurement, even for tiles in motion, the system allows to control the whole production in-line, without any intrusivity. The use of mercury is limited to the calibration step. Therefore, the proposed measurement method has a significant impact on the process control and on quality and safety control.

Theory

The time of flight of an ultrasonic wave depends, given a certain length of the propagation path, on the propagation velocity in the medium. In an isotropic material, the relationships between longitudinal (oscillation along the propagation direction) waves velocity v and transversal (oscillation orthogonal to the propagation direction) waves velocity v_t with the elasticity properties of the material are given by [9]:

$$v = \sqrt{\frac{E}{\rho} \cdot \frac{(1-\mu)}{(1+\mu)\cdot(1-2\mu)}} \tag{4}$$

$$v_t = \sqrt{\frac{E}{\rho} \cdot \frac{1}{2(1+\mu)}} = \sqrt{\frac{G}{\rho}} \tag{5}$$

where E is the Young's modulus, G is the elasticity tangential modulus, μ is the Poisson coefficient and ρ is the density of the material. For a porous body, like a green tile (isotropic in first approximation, as obtained by powder compaction), there are many theoretical models linking the elastic properties with porosity and consequently with the apparent density [10]. Commonly for ceramic bodies, the empiric Spriggs model is used [11], which states that Young's and elasticity tangential modules exponentially decrease with porosity:

$$E = E_0 e^{-bp} \tag{6}$$

$$G = G_0 e^{-bp} \tag{7}$$

where E_0 and G_0 are the values at null porosity (p=0, ρ=ρ_s), and b is a parameter to be experimentally determined, which can differ by some percentage between equations (6) and (7), but it is normally b=4.0–4.5 when p=0–40%.

The Poisson coefficient μ tends to decrease with the apparent density too, but its variation (in particular, in the considered range for a green tile, i.e. μ=0.1–0.2) can be considered as negligible in comparison with the variation of Young's modulus [5]. In [12], accurate experimentations and simulations showed that the variations of μ are in a range of 0.01 for a 50% porosity reduction. Moreover, supposing an isotropic material, μ is proportional to the ratio between E [equation (6)] and G [equation (7)], which is, in practice, constant with porosity. Therefore, in this paper, it is assumed that the Poisson coefficient is invariant with the apparent density. This hypothesis, supported by theoretical and empirical observations, is important for the industrial application of the proposed method, as it allows elimination of equation (5) in which v_t is not easily measurable with non-contact ultrasound probes (especially in-line).

Considering only the longitudinal wave velocity, like those propagated by a non-contact ultrasound probe that measures orthogonally to the sample surface, the relationship that links the velocity v and the apparent density ρ is obtained by combining equations (3), (4) and (6):

$$v = \sqrt{\frac{E_0 \cdot e^{-b\cdot\left(1-\frac{\rho}{\rho_s}\right)}}{\rho} \cdot \frac{(1-\mu)}{(1+\mu)\cdot(1-2\mu)}} \tag{8}$$

In Fig. 1(a), the function of equation (8) is plotted for typical values (e.g. [10]) for ceramic green tiles (E_0=6 GPa, b=4, μ=0.2, ρ_s=2,600 kg/m^3) obtained by traditional mix of raw materials (clays, feldspars, etc.) and with a fixed constant humidity content. The graphic shows that, increasing the apparent density up to porosity values lower than 60% (i.e. about ρ>1,000 kg/m^3), the longitudinal wave velocity tends to increase with an almost linear

trend. If a typical range of apparent density of industrial interest is considered [Fig. 1(b)], linearity constitutes a good approximation. In fact, the discrepancies between the model's data and their linear interpolation are always lower than 2 m/s (i.e. lower than 0.2%).

Figure 2 provides the results of a parametric analysis of equation (8) with the variation of E_0, b and μ. This analysis clearly shows that the uncertainty on the model parameters can generate significant uncertainty on the results of the correlation between velocity and apparent density. On the contrary, the discrepancies caused by the linearization seem to be always very low.

The Measurement Method and the Experimental Apparatus

In the proposed measurement method, the time of flight of ultrasound waves is measured with non-contact probes in transmission configuration through the tile in the production line. The scheme of this measurement method is showed in Fig. 3.

First of all, the distance among the probe membranes D (100 mm in this case) has to be measured using a caliper. It follows that the ultrasound measurement method consists in two steps: (a) measure the time of flight t_a of the ultrasound wave in air in the environmental condition of use; (b) measure the time of flight of the ultrasound wave through the tile body t_c (where $t_c<t_a$). Through measurement of the arrival time of the second echo, it is possible to know also the time of propagation t_m of the wave inside the material. These steps are repeated every time a tile passes through the probes during the production.

The time of flights are measured with cross-correlation algorithms between the excitation signal of the transmission probe and the received signal. A typical signal of cross-correlation measured on a green tile is showed in Fig. 3(c): t_c is represented by the first peak, whereas the difference in the time axis between the first and second peak represents $2t_m$.

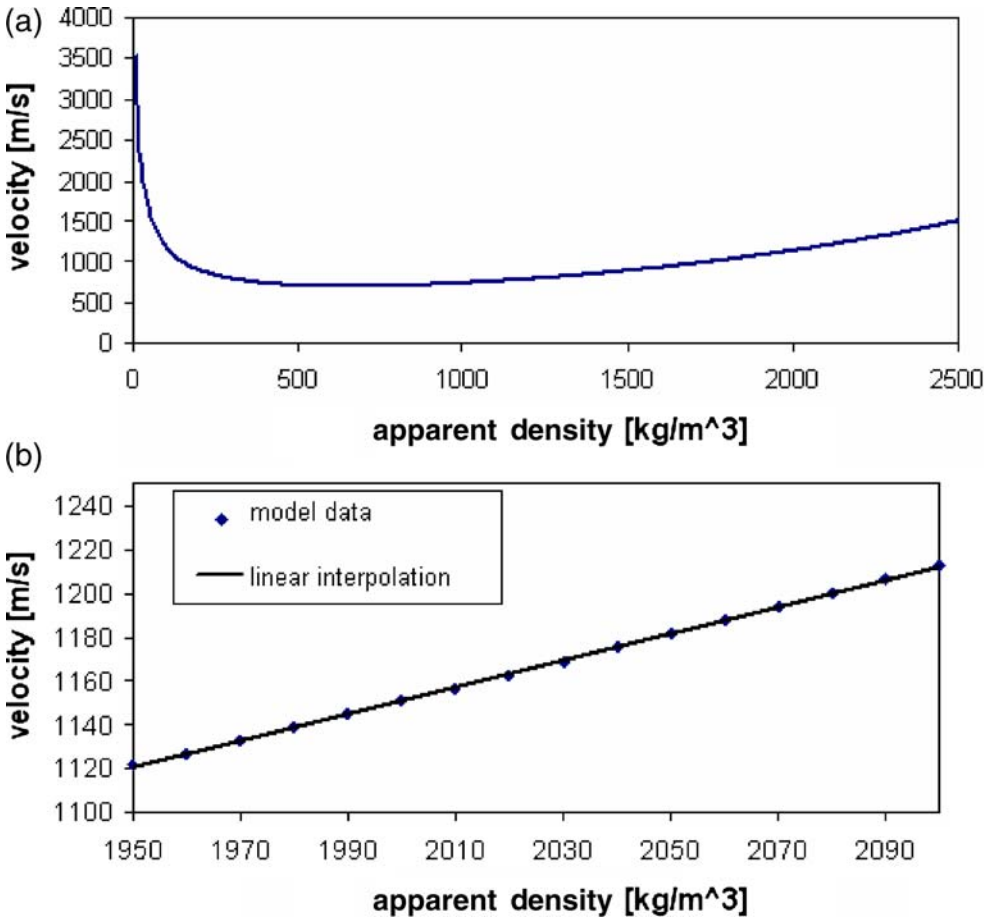

Fig. 1 (**a**) Plot of the longitudinal waves velocity v as a function of the apparent density (E_0=6 GPa, b=4, μ=0.2, ρ_s= 2,600 kg/m^3); (**b**) zoom of the diagram in a typical range of industrial interest with relative interpolating straight line

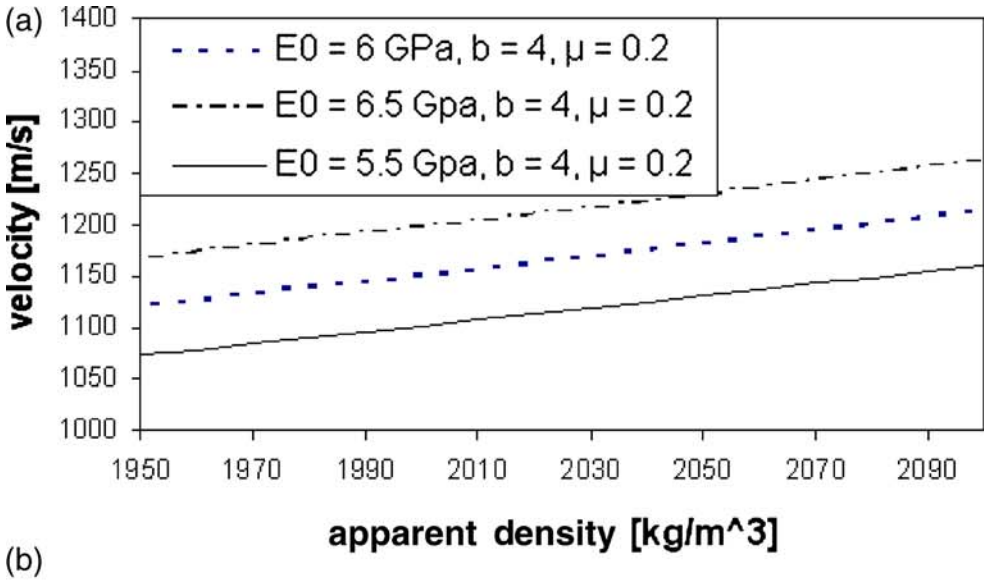

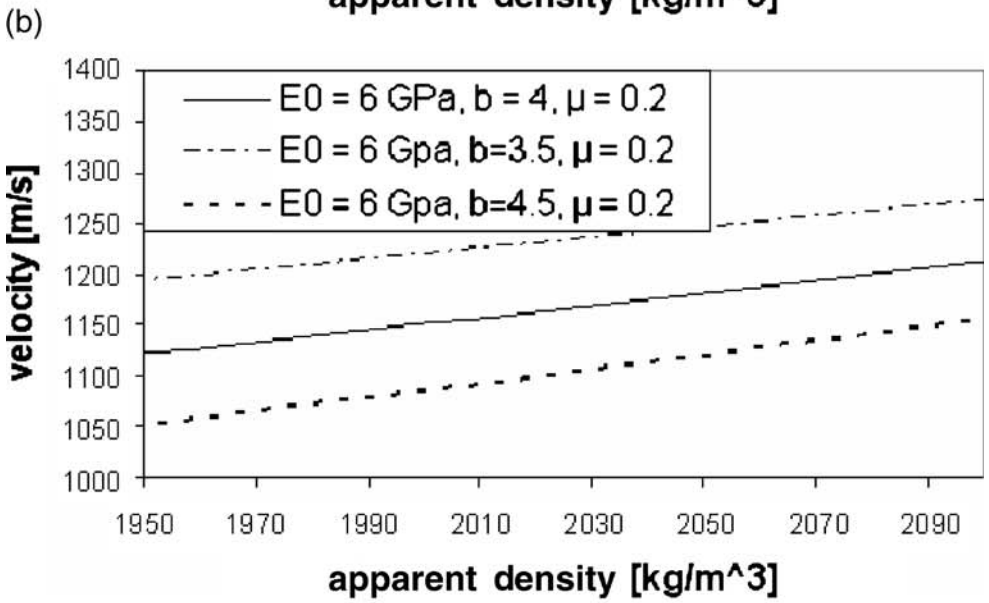

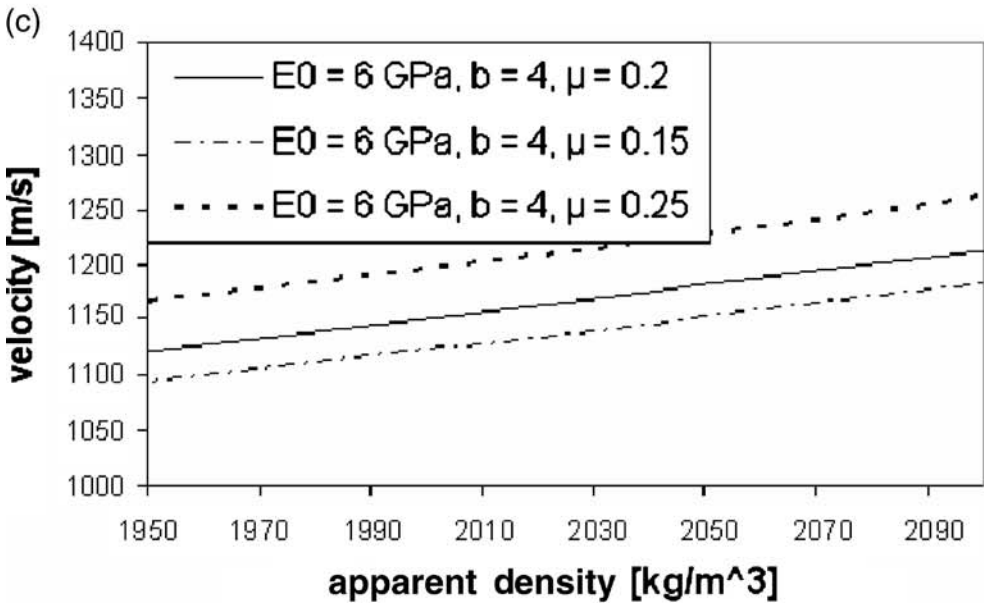

Fig. 2 Parametric analysis of equation (8) as a function of: (**a**) Young's modulus E_0; (**b**) empiric coefficient b; (**c**) Poisson coefficient μ

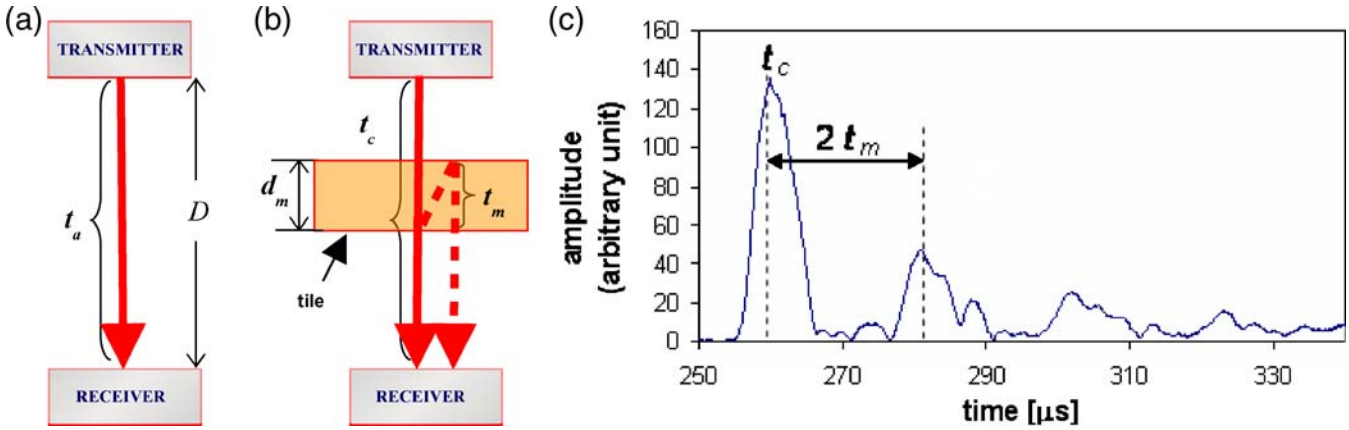

Fig. 3 Scheme of the measurement method: (**a**) measurement in air, (**b**) measurement on the tile, (**c**) example of cross-correlation signal measured on a tile (amplitude in arbitrary unit)

From the measurement in air, it is possible to obtain the propagation velocity of sound in air under a given environmental condition:

$$v_a = \frac{D}{t_a} \tag{9}$$

It is necessary to often repeat this measure because, as well known, the sound velocity v_a changes in environmental condition mainly as a function of temperature and humidity. For example, with a temperature of 20°C and with a relative humidity of 50%, there is a speed of 344 m/s.

In the literature, there are many formulas for the sound velocity estimation; for example, from [13]:

$$v_a(T,\theta) = (331.5 + 0.59 \cdot T[^\circ C])\left(1 + 0.004\frac{\theta[\%]}{100}\right) \tag{10}$$

where T is the air temperature and θ is the relative humidity.

Nevertheless, to avoid the measurement of temperature and humidity, it is better to compensate this effect by directly measuring v_a, especially in the production line where it is difficult to control environmental conditions.

By measurement of t_c and t_m, the average thickness of the tile in the area of the ultrasonic beam (about 1 cm^2) can be obtained

$$d_m = D - v_a(t_c - t_m) \tag{11}$$

and, in the end, the propagation velocity of longitudinal waves can be obtained as:

$$v = \frac{d_m}{t_m} \tag{12}$$

In reality, also the humidity content may have an influence on the propagation velocity, but this has not been considered in the present work as measurements have been performed on dried tiles or on tiles with constant humidity level. A preliminary attempt to deal with the humidity influence on such ultrasonic measurements has been, however, recently presented in [14].

The experimental apparatus used in the present work is based on piezoelectric probes with a diameter of the membrane of 12.5 mm working at around 1 MHz. These probes [15] have a dedicated layer of low impedance material (porous plastic, pressed fibres, polymers, etc. depending on the specific patent) placed between the piezoelectric crystal and the air to reduce the impedance difference between emitting element and air. In fact, the attenuation of the energy transmitted at the interface between two mediums is proportional to the square of the difference between the acoustic impedance of the two mediums. This phenomenon not only takes a low emission efficiency, but it limits also the energy of the wave propagating in the material. For example, the signal attenuation on an aluminium sample is 20 dB when the measurement is in water, whereas this increases to 158 dB when the measurement is in air! If, finally, also the effect of attenuation in air is added, it is clear how non-contact measurements could be very critical in terms of SNR, especially at the highest frequencies (>1 MHz) where these phenomena are stronger.

The probes are controlled by the NCA-1000 unit, constituted by a PC with dedicated boards for the generation of high-voltage ultrasonic signals, necessary to actuate the non-contact probes. The analog signals were acquired by a LeCroy LA340 oscilloscope (maximum frequency 1 Gs/s, vertical resolution 8 bit); the signals were then processed in the LabView environment. This measurement chain allows to obtain an *efficiency* (defined

as 20 $\log_{10} V_{\text{received}}/V_{\text{emitted}}$) "just" 40 dB lower than a traditional contact system.

The signal used to excite the probes is a chirp, whose amplitude, duration and frequency have been optimized during the study to maximize the SNR. In this work, a $\text{SNR} = 24 \div 28\ dB$ was obtained with 200 averages in different test conditions using the following parameters for the excitation signal:

- Central frequency, 950 kHz
- Band amplitude around the central frequency, ±280 kHz
- Duration, 350 μs

As previously shown (Introduction), the propagation velocity is proportional to the apparent density ρ, the quantity of interest for the present work. Once the velocity is measured, equation (8) could allow determination of ρ; nevertheless, it would be also necessary to know E_0, b, μ and ρ_s. Considering that those parameters change by tile typology (body, raw materials, etc.), their measurement is very complex and uncertain and that this uncertainty can reduce the accuracy in the density determination (see Fig. 2), it is not suggested to use equation (8) to measure ρ for the purposes of the present work.

On the contrary, considering that in the range of interest, equation (8) can be considered as linear with an error lower than 0.2%, this paper proposes to find the linear experimental correlation between velocity and apparent density. This relationship can be obtained by an experimental calibration procedure to be carried out with a reference method of known uncertainty, such as the one based on mercury. Once the relationship is determined, the ultrasound system can be used to measure density in-line.

In this way, a simple, robust method is obtained to be applied in industrial field, based on an experimental relationship specific for the examined material, without uncertainty on the estimation of model parameters.

In this work, green ceramic tiles having flat faces on both sides, produced in laboratory, have been used as calibration samples. The planarity of the sides allows to have a higher SNR (see next paragraph) because the grid in the rear side of the tile represents a modifying input for the ultrasound measurement, caused by the effects of diffraction and thickness variations. In addition, the samples have been dried to avoid any effect due to moisture. For the calibration, 20 samples of known density (five samples for four different pressing levels) were used. The propagation velocity is measured in a point of each sample with 200 averages on the signal. Figure 4(a) provides an example of correlation diagram, which can be later used to determine the apparent density of unknown samples, once the propagation velocity is measured. It is worth to underline that the determined parameters are valid only for ceramic green tiles with body and raw materials used for the calibration samples. In industrial field, it is necessary to repeat the calibration with every change of body. Such correlation has been extensively verified in the research work on different raw material typologies, and it is completely supported by the theoretical model that justifies the linearization in the considered range. Examples of correlation diagrams achieved for three different kinds of clay and body are reported in Fig. 4(b), showing the possibility of generalizing the method.

Uncertainty Analysis

The measurement of the apparent density with the proposed method consists of three main steps (once the distance D between the probes is fixed and measured):

Step 1. Times of flight measurement
Step 2. Estimation of the longitudinal waves velocity through equations (11) and (12)
Step 3. Experimental correlation between velocity and apparent density through calibration

In each step, there are uncertainty components that could be generated and propagated up to the final results. To optimize the measurement process, it is necessary to determine in detail the weight of each uncertainty source on the final results.

The measurement of the times of flight (Step 1) is mainly affected by repeatability problems. In fact, as previously shown, the measurement in air has important energy losses in the signal caused by the relevant differences of impedance between the propagation mediums. The non-contact ultrasound probe signal can be unstable and noisy ($\text{SNR} = 24 \div 28\ dB$ in this case), even though the measurement setup and the acquisition system are optimized for the use. It is obviously possible to increase the number of averages to reduce the noise, but in this case, this possibility is limited by the time available for the on-line measurement. Table 1 shows the results of standard uncertainty estimation obtained with N=1,000 repeated measurements on the same sample. Even in that case, 200 averages were carried out for each measure.

Considering that the duration of the excitation chirp signal is 350 μs and that after another 350 μs, all the following echoes completely disappear (i.e. are definitely covered by the noise) because of the strong losses at the interfaces and the attenuation in air, it was decided to generate a chirp every 700 μs. The total time for each measurement with 200 averages is thus about 0.14 s such as it could be performed on-line. From the results, it is clear that the grid on the rear side of the tile reduces the repeatability; this is due to diffraction effects, curvatures

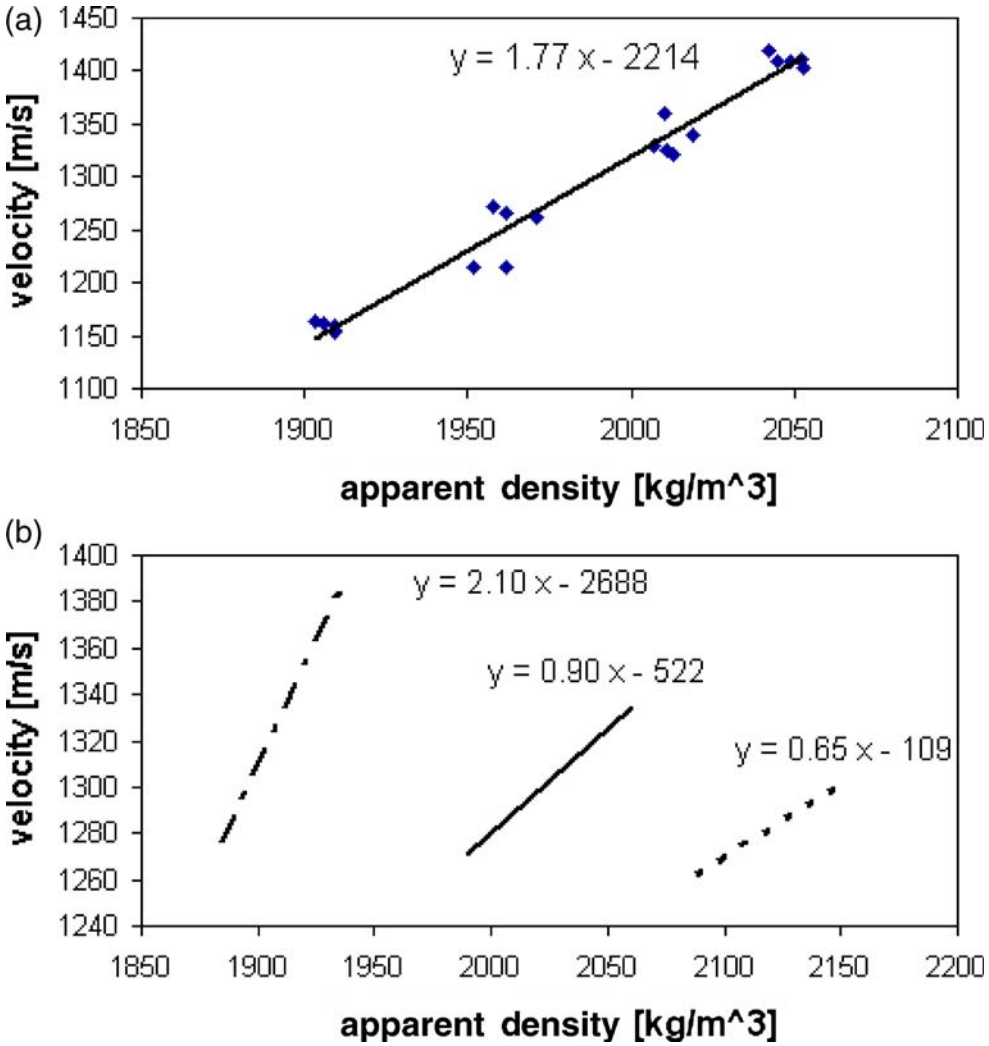

Fig. 4 (**a**) Correlation diagrams (with relative straight fitting line) between longitudinal wave velocity and apparent density measured on green ceramic tiles; (**b**) examples of correlation diagrams achieved on green tiles with different raw materials and body

and thickness variations that tend to further disperse the ultrasonic beam. Samples with flat sides and tiles with grid have been clearly realised with the same raw materials.

A low repeatability in the measurement of times of flight propagates into the velocity estimation (Step 2) through equations (11) and (12).

Table 1 Estimation of type A standard uncertainty in the measurement of times of flight with N=1,000 repeated measurements

Example of typical measured values	Standard uncertainty	
	Tiles with flat faces on both sides	Production tiles with the grid on the lower side
t_c=260.28 μs	$u_s(t_c)$=0.066 μs	$u_s(t_c)$=0.091 μs
t_m=7.50 μs	$u_s(t_m)$=0.035 μs	$u_s(t_m)$=0.085 μs
t_a=277.78 μs	$u_s(t_a)$=0.035 μs	$u_s(t_a)$=0.035 μs

To assess such propagation, the expression of combined uncertainty [16] for the propagation velocity v was used, which in this case is:

$$u(v) = \sqrt{\begin{aligned}&\left(\frac{t_a - t_c + t_m}{t_a \cdot t_m}\right)^2 \cdot u^2(D) + \left(-\frac{D\cdot(t_a - t_c)}{t_a \cdot t_m^2}\right)^2 \\ &\cdot u^2(t_m) + \left(-\frac{D}{t_a \cdot t_m}\right)^2 \cdot u^2(t_c) \\ &+ \left(\frac{D\cdot(t_c - t_m)}{t_a^2 \cdot t_m}\right)^2 \cdot u^2(t_a) + 2\cdot\left(-\frac{D\cdot(t_a - t_c)}{t_a \cdot t_m^2}\right) \\ &\cdot\left(-\frac{D}{t_a \cdot t_m}\right)\cdot u(t_m)\cdot u(t_c)\cdot r(t_m, t_c)\end{aligned}} \tag{13}$$

In this estimation, also the possible correlation between t_c and t_m was considered, as these are quantities simultaneously extracted from the same cross-correlation signal. An experimental analysis carried out on different tile typologies shows that $r(t_m, t_c)$=−0.1 to −0.4 [see example

in Fig. 5(a)]. The correlation between the two variables is mostly caused by the fact that the instantaneous oscillations of the ultrasonic beam, emitted by the vibrating membrane, took minimal variations of dimension and direction of the very beam. These variations are observed by the measurement system as an instantaneous minimal variation of the thickness d_m, which is not perfectly constant also in the samples with flat sides. To prove it, if from equations (11) and (12) the relationship between the two variables is obtained under the hypothesis that only the material's thickness changes [t_a, v and v_a are constant, whereas t_m changes with d_m in accordance with equation (12)], the following equation can be achieved:

$$t_c = t_a + \left(1 - \frac{v}{v_a}\right) \cdot t_m \tag{14}$$

Figure 5(a) provides this function diagram overlapped to the experimental data to show the similitude in the observed trend. Further confirmation of this hypothesis is that the correlation coefficient in module is higher in tiles with the grid.

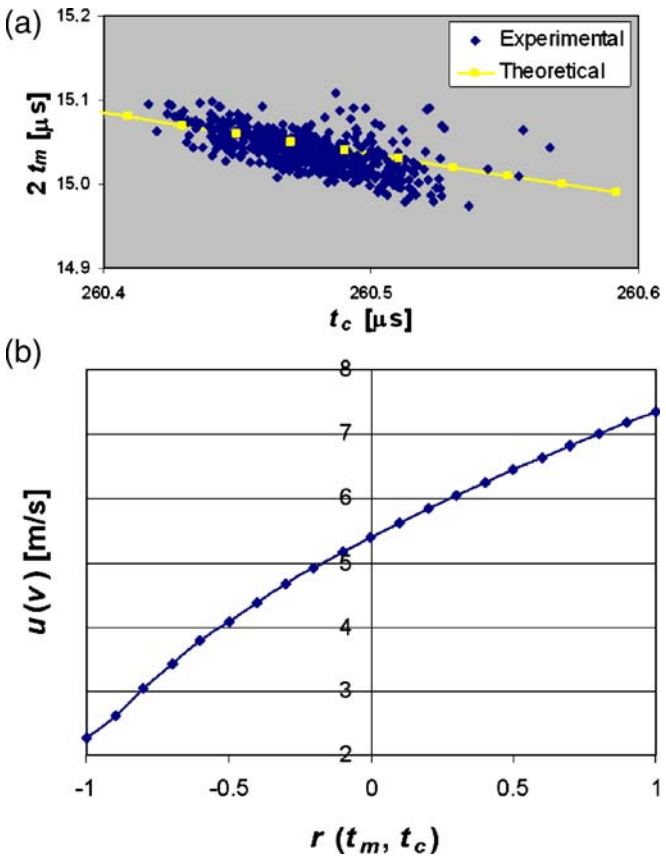

Fig. 5 (**a**) Correlation analysis between t_c and t_m achieved on a sample with flat sides: $r(t_m, t_c)=-0.27$, compared with theoretical data from equation (14); (**b**) diagram of the standard uncertainty of v in function of the correlation coefficient $r(t_m, t_c)$ for tiles with flat sides (see Table 2)

Looking at the diagram [Fig. 5(b)] of the standard uncertainty $u(v)$ as a function of $r(t_m, t_c)$, it is clear that when $r(t_m, t_c)<0$, the standard uncertainty decreases with respect to the zero correlation case [i.e. $r(t_m, t_c)=0$]. This is very useful because in the tile with the grid, in which the repeatability is typically lower, it limits the uncertainty increase.

Nevertheless, considering the variation observed in $r(t_m, t_c)$, in this uncertainty analysis, it is preferred to assume $r(t_m, t_c)=0$ to have a sort of "safety coefficient" on the estimation.

Table 2 provides in a detailed way the obtained budget for the uncertainty sources [17]. The accuracy in the measurement of the probe distance (with a caliper) is evaluated in ±0.1 mm, taking into account also the potential effect of temperature and of the measurement procedure. The uncertainty on the peak assessment in the cross-correlation is estimated as ±5 ns (with a resolution of 1 ns) based on type B considerations [16] linked to the peak shape. Type A standard uncertainties are expressed with u_s (values from Table 1), whereas resolutions and accuracies evaluated as half-width of a rectangular distribution (whose variance value is thus estimated as $u_a^2/_3$) are reported in column u_a.

The analysis of the sensitivity coefficients c_j shows that t_m is the most influent factor, in opposition to D, which has a lower impact. Anyway, the repeatability uncertainty seems to be the most relevant. This suggests concentrating attention on the elaboration and "cleaning" of the signals. To this aim, in [18], the authors proposed algorithms for the noise filtering and reduction, especially during on-line measurements.

Finally, it is necessary to consider the uncertainty associated to the correlation between velocity and apparent density (Stage 3). To this aim, the slope of the experimental linear correlation achieved by calibration [Fig. 4(a)] has been considered, and from this, the apparent density standard uncertainty was derived as $u(\rho)=u(v)/1.77$. Table 3 provides the results. They are compared to the standard deviation S_ρ of the apparent density estimated by the least-squares interpolation of the experimental data of Fig. 4(a) for the tile with flat sides and of Fig. 7(b) for the tiles with the grid measured in-line during production. This value S_ρ can be considered as proportional to the whole accuracy of the method, whereas the value $u(\rho)$ is obtained as combined uncertainty from repeated measurements on a single sample and without considering the uncertainties on the coefficients of the linear interpolation.

The comparison and analysis of these results provide important information:

– The values are of the same order of magnitude; thus, the adopted model for the measurement method can be considered in first approximation as correct.

Table 2 Budget of uncertainty sources (without covariance) for tiles with flat sides

x_j			$u_s(x_j)$	$u_a(x_j)$	$u^2(x_j)$	$c_j = \frac{\delta v}{\delta x_j}$	$c_j^2 u^2(x_j)$
Symbol	Value	Description					
D (m)	0.10	Accuracy		1.0E−04	3.3E−09	1.2E+04	4.8E−01
t_a (s)	0.00028	Accuracy		5.0E−09	8.3E−18	4.4E+07	1.6E−02
		Repeatability	3.5E−08		1.2E−15	4.4E+07	2.3E+00
		Resolution		5,0E−10	8,3E−20	4,4E+07	1,6E−04
t_c (s)	0.00026	Accuracy		5.0E−09	8.3E−18	−4.8E+07	1.9E−02
		Repeatability	6.6E−08		4.4E−15	−4.8E+07	1.0E+01
		Resolution		5.0E−10	8.3E−20	−4.8E+07	1.9E−04
t_m (s)	7.5E−06	Accuracy		5.0E−09	8.3E−20	−1.1E+08	1.0E−03
		Repeatability	3.5E−08		1.2E−15	−1.1E+08	1.5E+01
		Resolution		5.0E−10	8.3E−20	−1.1E+08	1.0E−03
Variance of v							2.8E+01
Standard uncertainty $u(v)$ (m/s) for tiles with flat sides							5.3E+00
Standard uncertainty $u(v)$ (m/s) for tiles with the grid (achieved by a similar table, but considering the standard uncertainties u_s of Table 1 for the tiles with the grid)							1.1E+01

– The differences between $u(\rho)$ and S_ρ are due especially to two elements whose weight is up to 50% of the whole balance of uncertainty:
  (a) Non-uniformity in the calibration samples: this point is particularly critical because ρ is a "local" quantity that may have spatial variation even inside the same sample. The ultrasound method works in an area of about 1 cm^2, whereas the mercury method performs a sort of average on the whole sample volume (normally with a surface of 10 cm^2). This can cause a significant spread of the data.
  (b) Extension of the analysis to the whole range (and not only around a single value) with a consequent linearization uncertainty in the relationship between v and ρ.
– The expanded uncertainty with a coverage factor of 2 is compatible with the accuracy requirements of the industrial problems, thus showing the applicability of the proposed experimental correlation method.

Application in Production Line

Finally, the measurement system was installed (Fig. 6) and tested in the industry Leonardo 1502 Ceramica of Casalfiumanese (BO). In the production line, many different interfering and modifying inputs are present that have to be assessed. In particular:

1. Non-controlled temperature of the environment: the measurement of v_a allows to compensate this effect.
2. Powder on probes membranes.
3. Vibrations: to reduce the effect of this phenomenon, it has been decided to isolate at the base and separate the structure holding the probes from the structure of the line (from which vibrations are generated). This was imposed to have a support with a long rigid arm for each probe; this generates uncertainty in the value of D, which is not, however, very critical due to the low sensitivity of the method to the uncertainty on the probe distance (see Table 2) and alignment.
4. The tiles on the line have the grid embossed on the back side and often present superficial roughness for decorative purposes: these factors generate, as previously shown, thickness variation and diffraction effects.
5. The tile is in movement on the line: this imposes a dynamic modulation of the effects at point 4 with a frequency equal to the passing of each edge of the tile grid between the probes, thus increasing uncertainty. Algorithms for noise filtering and reduction have been proposed by Marchetti and Revel [18].

Table 3 Comparison of standard uncertainties achieved by the two different methods

	Standard uncertainty achieved by measurements on a single sample [$u(\rho)=u(v)/1.77$)]	Standard deviation of the linear regression of the experimental data over the whole range (S_ρ)
Tiles with flat faces	3.0 kg/m^3	6.1 kg/m^3
Tiles with the grid	6.2 kg/m^3	8.5 kg/m^3 (on-line data)

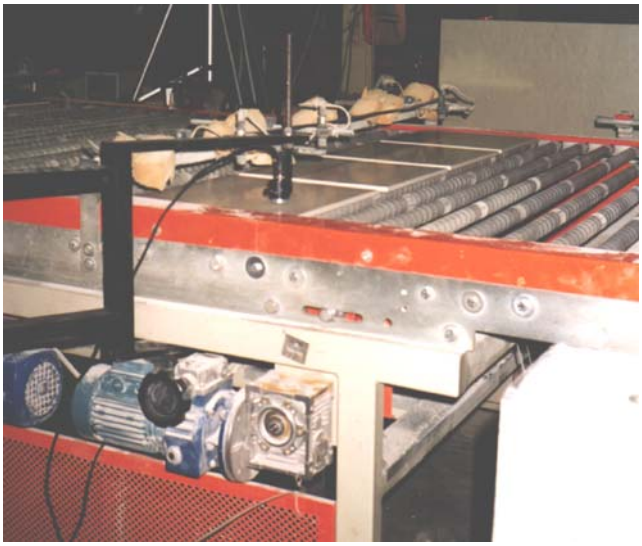

Fig. 6 Installation of the ultrasonic probes in the production line

Figure 7(a) provides an example of the result achieved after the drier. Each density value corresponds to the average on a line 6–7 cm long. The acquisition is synchronized with an optical sensor, which recognizes the presence of the tile. Some tiles, measured on the line with the ultrasound method, are then taken from the line and measured with the mercury reference method. The achieved results are synthesised in Fig. 7(b) and Table 3, showing thus the effectiveness of the proposed technique.

Conclusions

In this work, an original method for the measurement of the apparent density of ceramic green tiles during production has been developed and applied. The method, being based on non-contact ultrasonic probes, is completely non-

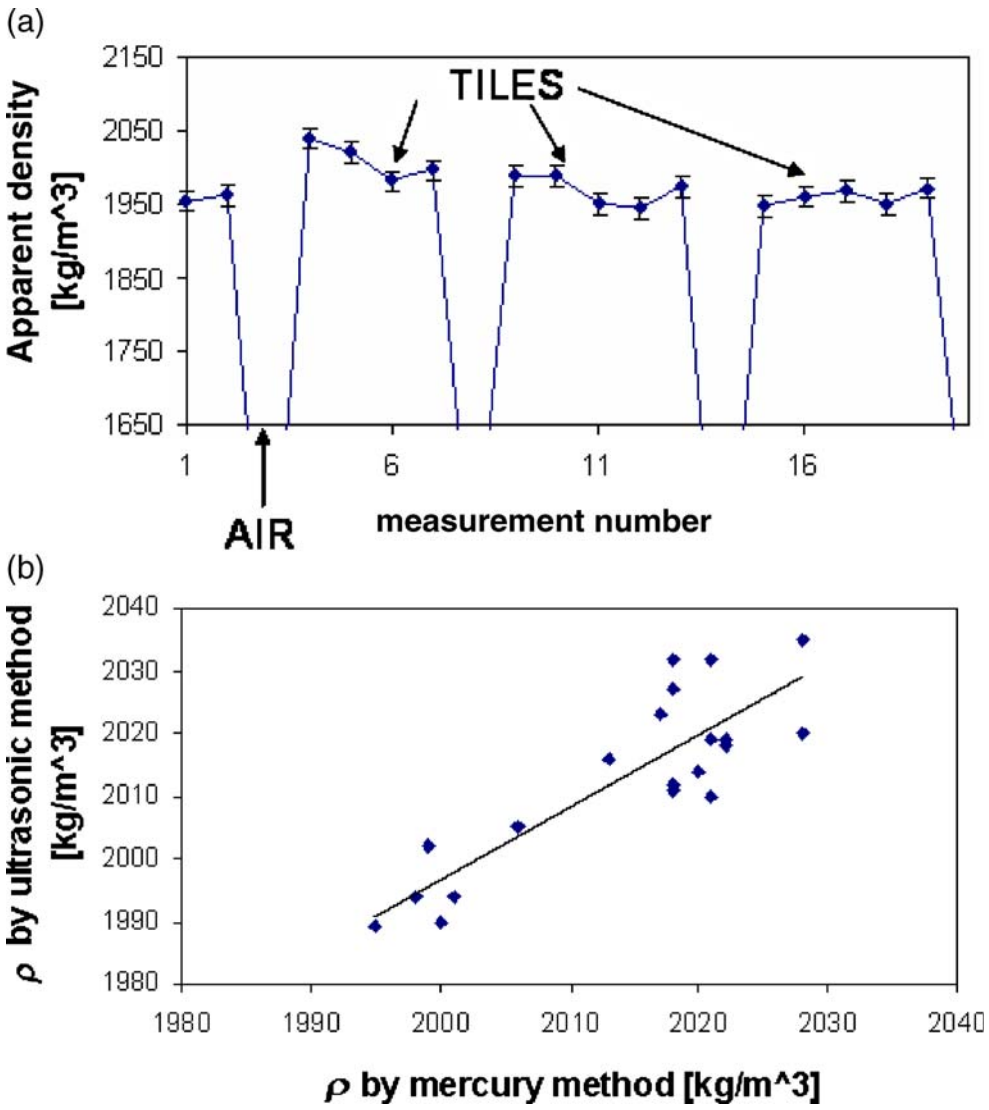

Fig. 7 (**a**) On-line measurement results with relative uncertainty bars; (**b**) comparison between on-line ultrasonic measurements and reference laboratory mercury measurements

intrusive assuring the opportunity to check the 100% of the production in real time. Moreover, the proposed technique allows to have information on the spatial distribution of the apparent density over the tile, an important parameter for the dimensional conformity of the tile after the firing.

The uncertainty analysis allowed to determine the achievable accuracy (about ±0.75% of the reading), which is compatible with the specific requirements of the industrial application. The experimental correlation between the velocity propagation and the apparent density has been verified in the work through experimental calibrations, and it is supported by the theoretical model that justifies the linearization in the considered range. A detailed uncertainty analysis was carried out to quantify the effect of this correlation procedure. It is shown that the main uncertainty sources are linked to measurement repeatability problems in air and to the limited uniformity of the calibration samples. In the end, an application of the measurement method in production line was presented, which confirms the achievement of the initial targets of the work.

Further development of this activity will be linked to the extension and application of the measurement method to other industrial sectors with similar problems, such as the wood and paper production.

Acknowledgments This research has been carried out within the SENSOCER project, funded by the European Commission in the 5° Frame Programme (*Standard, Measurement & Testing*, G6RD-CT2001-00637). The author would like to thank all the project's partners. Finally, the author also thanks Dr. Paolo Pietroni for the useful discussions during the analysis of the results.

References

1. Dinsdale A (1986) Pottery Science: Materials, Process and Products. Chichester, Ellis Horwood. ISBN 0470202769.
2. Amoros JL (1987) Pastas ceramicas para pavimentos de monococcion. Influencia de la variables de prensado sobre las propriedades de la pieza en crudoy sobre su comportamiento durante el prensado y la coccion. PhD Thesis, University of Valencia, 61.
3. Standard UNI EN 1097-3 (1999) Determinazione della massa volumica in mucchio e dei vuoti intergranulari, ICS 91.100.15.
4. Pei P, Minor D, Onoda G (1999) Laboratory techniques for bulk density measurements, Chapter 17. In: Jillavenkatesa Da A, Onoda G (eds) Advances in process measurements for the ceramic industry. Westerville, OH, pp 293–306, ISBN 1574980866.
5. Enrique-Navarro JE, Garcia J, Amoros JL, Beltran V (1998) Alternatives to immersion in mercury for determining tile bulk density. Interceram, 47(1) ISSN 0020-5214.
6. Sheppard LM (1998) Measurement advances for ceramic processing control. Ceramic Industry, 60, October, ISSN 0009-0220.
7. Engmann D (2000) Quality testing of green ceramic tiles: measurement principles for determining bulk density. Interceram 49(4):250, ISSN 0020-5214.
8. Bhardwaj MC (1997) Innovation in non-contact ultrasonic analysis: applications for hidden objects detection. Mat Res Innovat 1:188–196, ISSN: 1432–8917.
9. Krautkramer J, Krautkramer H. (1983) Ultrasonic testing of materials. Spinger-Verlag, Berlin, ISBN 3-540-11733-4.
10. Wachtman JB (1996) Mechanical properties of ceramics. Wiley, New York, ISBN: 0-471-13316-7.
11. Spriggs RM (1961) Expression for effect of porosity on elastic modulus of polycrystalline refractory materials, particularly aluminium oxide. J Am Ceram Soc 45:94, ISSN 0002-7820.
12. Roberts AP, Garboczi EJ (2000) Elastic properties of model porous ceramics. J Am Ceram Soc 83(12):3041-3048, ISSN 0002-7820.
13. Cramer O (1993) The variation of the specific heat ratio and the speed of sound in air with temperature, pressure, humidity, and CO_2 concentration. J Acoust Soc Am 93(5):2510–2616, ISSN 0001-4966.
14. Cantavella V, Llorens D, Mezquita A, Moltò C, Bhardwaj MC, Vilanova P, Ferrando J, Maldonado-Zagal S (2006) Use of ultrasound techniques to measure green tile bulk density and optimise the pressing process. Proceedings of QUALICER 2006, February, Vol. 2, P.BC-161, ISBN 84-95931-21-4.
15. Bhardwaj MC (2002) High transduction piezoelectric transducers and introduction of non-contact analysis. In: Harvey JA (ed) Chapter of Encyclopedia of Smart Materials. Wiley, New York, ISBN 0-471-17780-6.
16. ISO (1993) Guide to the expression of uncertainty in measurement. ISO, Geneve, ISBN 92-67-10188-9.
17. Barbato G (2002) Misurare per Decidere, Ed. Esculapio, Bologna, ISBN 88-86524-76-5.
18. Marchetti B, Revel GM (2003) On line density measurement on green ceramic tiles. Tile & Brick International, ed. DVS-Verlag Gmbh, Dusseldorf, Germany, 19(1):4–12, ISSN 0938-9806.